AI-Driven Detection/Classification of High Impedance Faults in Low Voltage Distribution Networks Using Sliding DFT and Deep Neural Networks

Basem Abd-Elhamed Rashad[1]*

ABSTRACT

Abstract— High impedance fault (Hi-ZF) detection/classification in low voltage distribution networks remains a significant challenge due to the low fault current levels, which are often indistinguishable from normal load conditions using conventional overcurrent protection devices. Hi-ZF, typically caused by broken conductors contacting high-impedance surfaces such as soil or vegetation, pose serious public safety hazards, risk of fire ignition, equipment damage, and legal liability. This paper proposes a novel AI-driven detection/classification framework combining Sliding Discrete Fourier Transform (SDFT) and Deep Neural Networks (DNN) to accurately detect/classify both low impedance faults (LIFs) and Hi-ZFs using single-ended current measurements. The method first applies SDFT to extract frequency-domain features from local current signals. These features are then fed into a DNN classifier trained to distinguish between Hi-ZFs, LIFs, and non-fault transient events such as load/capacitor switching. The proposed scheme was validated using extensive simulations on the unbalanced IEEE 13-Bus distribution test system, employing ATP/EMTP and MATLAB/Simulink platforms. Results demonstrate that the scheme reliably detects Hi-ZFs and LIFs within 26.5 ms, achieving a classification accuracy of 99.1%, and the proposed AI-based methodology shows strong potential for enhancing protection and situational awareness in modern smart distribution grids.

Keywords: Distribution Network, Deep Neural Networks (DNN), Fault Detection/Classification, High impedance fault (Hi-ZF), Sliding Discrete Fourier Transform (SDFT)

I. INTRODUCTION

The growing complexity of modern power distribution networks, especially with the increasing integration of distributed energy resources, has significantly elevated the need for intelligent and reliable protection mechanisms. Among the various faults that threaten the safety and stability of these systems, high impedance faults (Hi-ZFs) remain particularly elusive. Such faults occur when conductors contact high-resistance surfaces (e.g., dry soil or vegetation) [1-2]. Due to their inherently low fault current magnitudes often similar to or lower than normal load currents Hi-ZFs typically fail to trigger conventional protection devices such as fuses or overcurrent relays, resulting in serious safety risks including arcing ignition, prolonged energized conductors, and undetected fire hazards [2-3].

A range of traditional techniques has been proposed to tackle Hi-ZF detection. Early approaches largely relied on signal processing-based analyses such as harmonic detection, total harmonic distortion (THD), and waveform distortion metrics to capture the nonlinear characteristics introduced by arcing faults [4].

[1] Department of Electrical Power and Machines Engineering, Higher Institute of Engineering at El-Shorouk City, El-Shorouk Academy, Cairo 11837, Egypt

* Corresponding Author: **Basem Abd-Elhamed Rashad** (e-mail: b.rashad@sha.edu.eg) (**BAR**)

Harmonic content analysis, for instance, has shown that Hi-ZF conditions often introduce distinct frequency-domain signatures, notably in the third and fifth harmonics [5]. Wavelet transform-based methods have improved time-frequency localization, offering insights into transient events associated with arcing [6]. Energy-based metrics have also been introduced to monitor shifts in signal intensity across various frequency bands [7][8]. However, many of these methods suffer from key limitations, including sensitivity to system noise, poor generalization across operating conditions, and overreliance on fixed thresholds, which limit adaptability and robustness [4][5][8].

To overcome these challenges, machine learning (ML) and deep learning (DL) techniques have emerged as powerful tools capable of learning complex, nonlinear fault patterns directly from raw or pre-processed electrical signals. Early ML methods, such as Support Vector Machines (SVM), Decision Trees, and Random Forests, showed improvements in both feature selection and classification accuracy for Hi-ZF detection [9]. For instance, Carvalho et al. [3] applied a threshold-based detection algorithm combined with Random Forest classification to handle Hi-ZF detection under varied fault scenarios. However, these techniques remained highly dependent on manual feature engineering and shallow model architectures, which constrained their scalability and flexibility.

In contrast, deep learning approaches, particularly Deep Neural Networks (DNNs) and Convolutional Neural Networks (CNNs), have shown significant promise in automating feature extraction and improving classification performance [10][11]. Rai et al. [10] proposed a convolutional autoencoder architecture that successfully learned the underlying representations of Hi-ZF signals from waveform data, thereby enhancing detection accuracy. Abasi-Obot et al. [11] extended this work by implementing a fully connected convolutional architecture capable of detecting and localizing Hi-ZF events simultaneously. The ability of DL models to generalize across diverse operating conditions has made them effective in addressing Hi-ZF variability.

Yet, the effectiveness of any AI-based classifier is critically dependent on the quality of input features. Time-frequency signal preprocessing remains essential to accurately represent the transient dynamics of fault events. Traditional Fourier methods, while useful for steady-state analysis, often lack temporal resolution. Although wavelet transforms provide better time-frequency localization, their implementation complexity can limit their use in real-time protection applications [12]. A more suitable alternative for real-time streaming environments is the Sliding Discrete Fourier Transform (SDFT), which enables sample-by-sample spectral analysis with low computational overhead. SDFT's continuous updating mechanism supports effective tracking of spectral changes, making it ideal for capturing the frequency-domain signatures of evolving fault conditions [12-14].

Abasi et al. [11] showcased the potential of SDFT for Hi-ZF detection using a discrete, non-recursive computation model. These works affirm the feasibility of SDFT as a real-time feature extraction tool. Rodrigues et al. [12] further demonstrated its effectiveness in classifying power quality disturbances in distribution networks. However, many existing studies using SDFT do not fully explore its integration with advanced DL classifiers or address the dual challenge of detecting both Hi-ZFs and LIFs under realistic non-fault transient scenarios such as load switching, capacitor energization, or motor starting [4][8].

This paper addresses this critical research gap by proposing a hybrid detection scheme that strategically combines SDFT-based spectral feature extraction with a DNN classifier. The aim is to achieve fast, accurate, and generalizable identification of both Hi-ZFs and LIFs using single-ended current measurements in low voltage distribution networks. The proposed approach is validated through extensive simulation on the unbalanced IEEE 13-Bus test system using ATP/EMTP and MATLAB/Simulink platforms, incorporating a wide range of fault types, inception angles, and system disturbances. The main contributions of this work are:

- Development of a real-time Hi-ZFs detection framework using *SDFT*-based spectral features and deep learning classification;
- Demonstrates the method's robustness and efficiency, achieving successful fault detection within 26.5 ms and a classification accuracy of 99.1%
- Comprehensive evaluation under various operating conditions, including different fault types, fault locations, fault inception angles and normal transient switching.
- The results confirm the effectiveness, robustness, and reliability of the proposed scheme in detecting Hi-ZFs and correctly distinguishing them from LIFs.

The remainder of this paper is structured as follows: **Section 2** presents the proposed methodology, including SDFT feature extraction and DNN architecture. **Section 3** details the simulation setup and case studies. **Section 4** discusses results and performance evaluation. Finally, **Section 5** concludes the paper and outlines future directions.

II. METHODOLOGY

The proposed methodology combines advanced signal processing with deep learning to enable fast, accurate, and intelligent detection of both Hi-ZFs and LIFs in low-voltage distribution networks. The detection framework consists of three main components: (i) signal acquisition and preprocessing, (ii) SDFT-based feature extraction, and (iii) deep neural network–based fault detection and classification. The overall system architecture is illustrated in Figure 1.

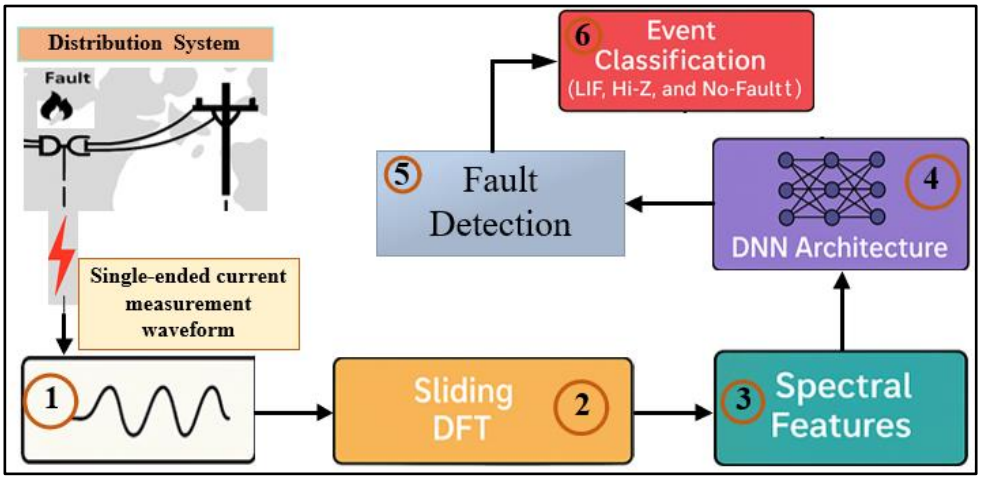

Figure 1. *System Architecture Block Diagram*

A. *Signal Acquisition and Preprocessing*

Current signals are measured at a single-end location (bus or feeder) using conventional current transformers (CTs). The time-domain signals are sampled at a high frequency (e.g., 10 kHz) to ensure adequate resolution for transient detection. No additional phasor measurements or synchronized data are required, making the method suitable for low-cost implementation and field deployment. The input signals are normalized to eliminate amplitude scaling effects and filtered with an anti-aliasing stage to remove high-frequency noise before processing.

B. *SDFT for Feature Extraction*

The Sliding Discrete Fourier Transform (SDFT) is applied to each sampled current signal to extract time-evolving frequency-domain features with high computational efficiency. Compared to the conventional DFT, SDFT facilitates real-time spectral tracking without the need to recompute the entire transform at each time step, thereby greatly reducing computational overhead [14]. For each observation window (typically one cycle in length, with sliding steps of one sample), the SDFT generates an amplitude spectrum from which characteristic features such as peak spectral energy and dominant frequency components are extracted. These features are particularly effective for capturing the subtle distortions introduced by Hi-ZFs and LIFs, which appear as localized variations in harmonic content [15]. Let us consider DFT computations in the time window of length M sliding along the signal X_n , such that $X_n = 0$ for $n < 0$:

$$x_n^k = \sum_{m=0}^{M-1} x_{q+m} W_M^{-km} \quad (1)$$

where $q = n - M + 1, 0 \le k \le M - 1$, and the complex twiddle factor equals $W_M = e^{J2\pi/M}$. In our notation the superscript k in x_n^k is not a traditional exponent but instead refers to the DFT' s frequency ($kth - bin$) index, and the subscript n is a time index. As such, k is a constant and the n in x_n^k indicates that the DFT is computed from samples $x_{n-M+1}, x_{n-M+2}, \ldots\ldots, x_n$. In the case of sample-by-sample signal processing, consecutive ($kth - bin$) DFT output samples $x_n^k, x_{n+1}^k, x_{n+2}^k \ldots\ldots$, are computed from the x_n time samples that differ only by the fi rst and last samples. A recursive formula for computing (1) may be derived as follows:

$$x_n^k = W_M^k \left(x_{n-1}^k - x_{n-M} + X_n\right) \quad (2)$$

The structure of difference in (2) is depicted in Figure.2. This traditional SDFT filter is only marginally stable because it has a z-domain pole located at $Z = W_M^k$ on the unit circle. This formulation enables real-time updates of frequency components with minimal latency and memory usage.

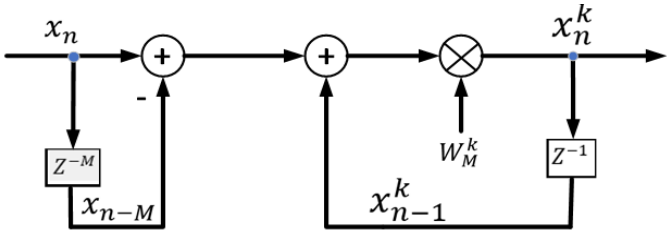

Figure 2. *Traditional SDFT structure*

C. DNN for Fault Detection/Classification

DNNs are employed to model complex nonlinear systems. Their computation is efficient, relying primarily on basic algebraic operations, which enables prompt response to fault conditions. The general architecture includes (i) an input layer matching the feature vector size, (ii) two to three hidden layers with ReLU activation functions, (iii) dropout layers for regularization, and (iv) a final SoftMax layer for multi-class classification [16]. The DNN developed for fault detection and classification in this study consists of an input layer with four neurons representing the maximum absolute values of SDFT features extracted from feeder currents of each phase and the ground current at the relay location. The premise of the proposed scheme is that feeder current measurements at the relay location can quickly indicate the presence of faults in the system.

The measurement data are first processed using the SDFT to extract relevant signal features. These features are subsequently fed into a DNN to detect and classify the type of fault. In cases where the fault is identified as unbalanced, an additional DNN module is applied to determine the affected phase. The resulting diagnostic information supports intelligent decision-making for downstream control actions, including fault isolation and system restoration. The SDFT features are illustrate the maximum absolute values of current-based SDFT features for each phase: $SDFT_a$, $SDFT_b$, $SDFT_c$, and $SDFT_g$. To confirm that all values lie within the range [0, 1], feature scaling can be utilized in the following form, as illustrated in (3), where (*I*) is the input vector: -

$$I' = \frac{I - min\ (I)}{max\ (I) - min\ \ (I)} \tag{3}$$

The nonlinear transformations are used in the hidden layers to convert the input data information into high-dimensional features. Here, $x = (2, \dots, d)$, $\bar{Y}$ is the hidden vector, $\bar{y}$ is the bias vector, W is the weight matrix and f is the activation function applied element-wise. The output of the final hidden layer is transformed using (4)

$$\bar{Y}_1 = f\,(W_1 . P + \bar{y}\,) \tag{4}$$

Three fully connected hidden layers were implemented, containing 20, 10 neurons and 5 neurons, respectively, activated using ReLU functions. The output layer includes two neurons corresponding to the detection/classification outputs: detection and classification, as illustrated in Figure 3, that present the visual representation of the suggested *SDFT-DNN*. This multi-layered structure ensures non-linear feature extraction and robust learning capabilities, distinguishing it from simpler machine learning models. Unlike conventional machine learning models such as linear regression or single-layer perceptrons, the Fault Detection/Classification based SDFT-DNN architecture leverages multiple hidden layers and non-linear activation functions to capture complex relationships between diverse input features and output detection/classification. At the final stage, the extracted spectral features are fed into a fully connected DNN trained to detect/classify events into one of three categories: Hi-ZFs, LIFs, and Non-Fault Events (e.g., load switching, capacitor energization).

In this study, a total of 1200 labeled samples were generated from the simulation studies under different operating conditions, fault types, inception angles, and different switching events. These samples were divided into 70% for training (840 samples), 15% for validation (180 samples), and 15% for testing (180 samples). To enhance robustness and prevent overfitting, several well-established techniques were employed: (i) applying five-fold cross-validation to ensure generalization across datasets, (ii) using dropout layers within the DNN to prevent co-adaptation of neurons, (iii) normalizing all input features to the range [0,1] for stable training, and (iv) ensuring balanced representation of Hi-Z faults, low-impedance faults, and non-fault events. These steps provided a reliable basis for training, validation, and evaluation of the proposed model. The model is trained using supervised learning on a labeled dataset generated from extensive simulations. The use of deep learning in this context allows for nonlinear decision boundaries, making the system robust against signal noise, parameter uncertainty, and waveform distortions outperforming traditional rule and threshold-based methods.

D. Fault Detection Flow

As noted above, DNNs a class of machine learning algorithms capable of capturing complex patterns and data relationships can be effectively applied for fault detection and classification in the studied system. A typical DNN architecture consists of four primary layers: (i) an input layer, (ii) multiple hidden layers, (iii) a SoftMax layer for probabilistic interpretation, and (iv) an output layer for final decision-making. The proposed detection scheme functions as a real-time decision

engine, as illustrated in Figure 1. Once the current waveform is received, the system: (1) applies SDFT on a sliding-window basis, (2) extracts spectral features, (3) inputs them into the trained DNN classifier, and (4) generates the detection/classification output.

The architecture of DNN is determined by several key design parameters, including the number and type of layers, the number of neurons within each layer, and the choice of activation functions. In this study, the DNN models for both fault detection/classification were developed using a dataset comprising 1200 samples obtained at the relay location. Of these, 840 samples were used for training, while 180 samples were allocated for testing and the remaining 180 samples for validation purposes. The objective of the proposed DNN is to identify both the presence and type of fault by analyzing features extracted through SDFT along with three-phase current measurements collected at the relay point. The detection/classification covers three categories: (i) LIFs, including single-line-to-ground (SLG), line-to-line (LL), double-line-to-ground (DLG), three-phase (LLL), and three-phase-to-ground (LLL-g) faults; (ii) Hi-ZFs, comprising single-phase and two-phase scenarios; and (iii) non-fault events, such as load switching and capacitor energization. The output layer of the DNN consists of four binary (0–1) indicators, each corresponding to a fault category. With this design, the proposed DNN can also distinguish normal operating conditions from fault scenarios, thereby effectively separating faulted and non-faulted events.

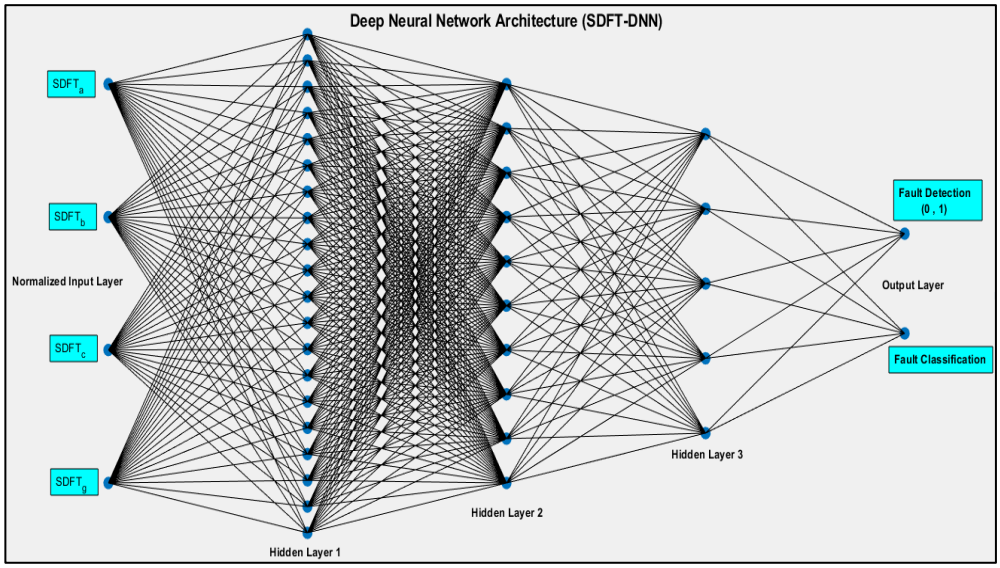

Figure 3. *Visual representation of the suggested SDFT-DNN*

III. SIMULATION SETUP AND CASE STUDIES

To validate the effectiveness and reliability of the proposed SDFT-DNN-based fault detection/classification scheme, comprehensive simulations were conducted on a low-voltage distribution system using both the ATP/EMTP and MATLAB/Simulink platforms. The simulation environment was configured to emulate realistic operating conditions, fault scenarios, and transient disturbances that occur in practical utility systems.

A. Test System Description

The simulations were conducted on the unbalanced IEEE 13-bus distribution test system, a

widely used benchmark for evaluating fault detection and protection algorithms in unbalanced low-voltage networks [17]. The system incorporates diverse load types, line configurations, and distributed capacitances, providing a realistic basis for assessing the scheme under varying operating conditions. Three-phase current signals were recorded at a single measurement point, located at the sending end of the protected feeder. This single-ended measurement approach reflects practical deployment scenarios, where phasor measurement units (PMUs) or synchronized data are often unavailable.

The performance of the proposed ***SDFT-DNN***-based fault detection and classification scheme was assessed using the unbalanced IEEE 13-Bus distribution test system, which includes a variety of scenarios such as Hi-ZFs, LIFs fault, and non-fault events including heavy load switching and capacitor bank energization. The system model was developed and simulated in the ATP/EMTP platform, as depicted in Figure.4.

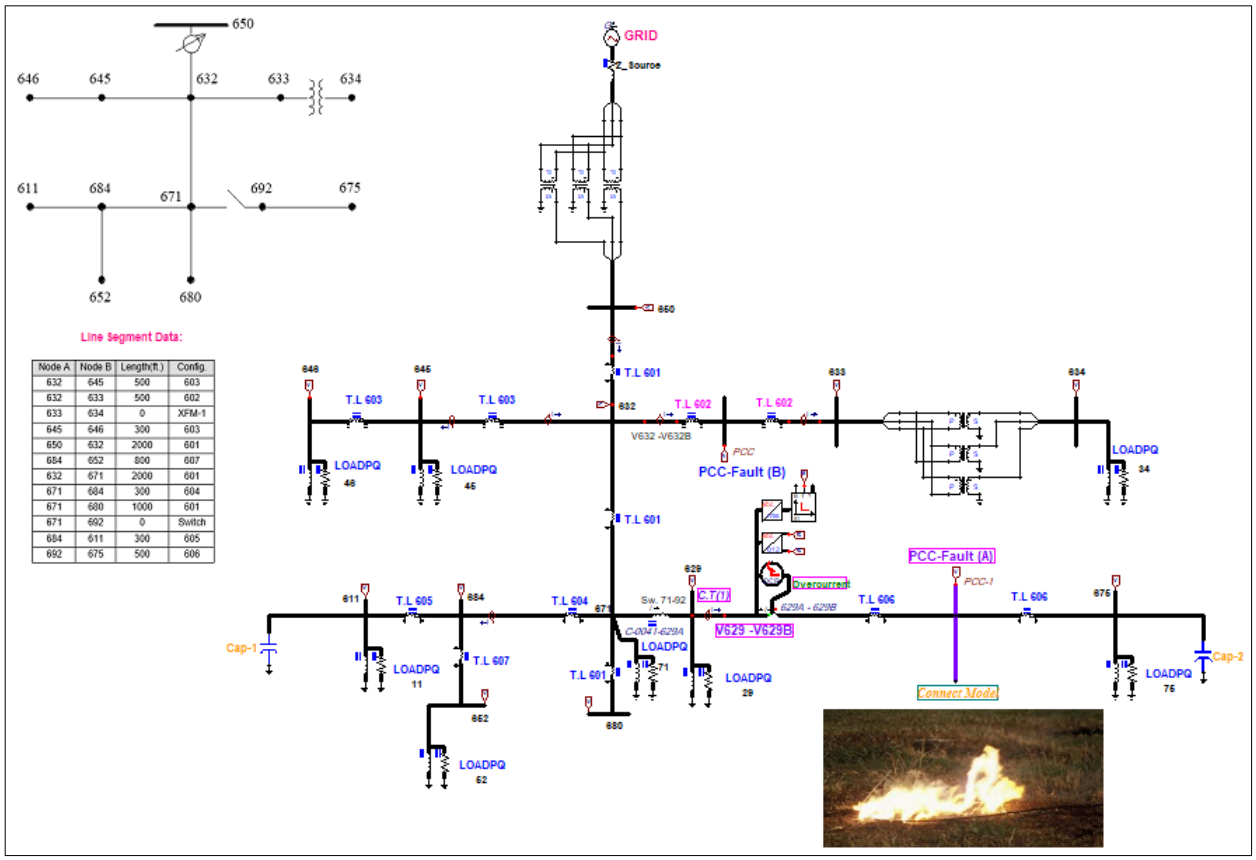

Figure 4. *ATP/EMTP unbalanced IEEE 13-Bus distribution test system*

The network is connected to the grid through a 200 kVA, 4.16 kV/25 kV step-up transformer rated at 100 MVA and operating at 50 Hz [18]. The IEEE 13-Bus system was selected for its unbalanced configuration and realistic representation of distribution network challenges. Transmission line parameters, load models, and fault scenarios were accurately configured to reflect both normal and abnormal system behavior. This setup allowed a comprehensive evaluation of the proposed DNN classifier's capability to accurately detect and differentiate Hi-ZFs, LIFs, and routine operating events. Testing was performed under diverse conditions to validate the classifier's robustness and generalization across electrical disturbances and operating states.

B. Hi-Z model

The Hi-ZF model used in this study is based on the Emanuel model, as described by Gomes et al. [19], and is illustrated in Figure 5(a). The ATP/EMTP Hi-ZF model under sandy soil conditions is shown in Figure 5(b). To replicate the typical waveform behavior of Hi-ZF currents, an anti-parallel diode configuration is utilized as illustrated in Figure 5(c). The voltage-current (V–I) characteristics of the Hi-ZF, shown in Figure 5(d), are generated by fine-tuning key model parameters: positive and negative arc voltages (V_p and V_n) and dynamic arc resistances (R_p and R_n). Notably, the modeled Hi-ZF is designed to simulate arcing behavior in sandy soil conditions, aligning with realistic fault scenarios reported in the literature [20-21]. The resulting current waveforms under Hi-ZF conditions exhibit distinct nonlinear and asymmetrical characteristics, often rich in SDFT features that aid in fault detection. To ensure robustness and generalization of the proposed detection scheme, a wide range of system conditions and fault variations were incorporated into the simulation framework, this comprehensive dataset forms the foundation for training and evaluating the proposed ***SDFT-DNN***-based detection/classification system:

- Fault Types: SLG: AG, BG, CG, DLG: ABG, BCG, CAG, LL: AB, BC, CA, LLL: ABC, and LLL-g: ABCg, in addition to Hi-ZFs involving one or two phases contacting high-resistance surfaces (e.g., dry soil).
- Non-Fault Events: Transient conditions such as load switching, capacitor switching, and normal operations with variable load levels.
- Fault Locations: Varied from 10% to 90% of the line length to emulate diverse fault distances from the relay point.
- Inception Angle: The current waveform's fault inception angle was varied from 0° to 330° in 30° increments, with Phase A is used as a reference.
- Fault Resistance: Adjusted between 0: 50 Ω for LIFs and 100:280 Ω for Hi-ZFs to cover different fault conditions.

IV. RESULTS AND DISCUSSION

This section presents the results obtained from the simulation of the proposed *SDFT-DNN-based fault detection/classification* system under a wide variety of operating scenarios, including both faulted and non-faulted events. The outcomes are analyzed in terms of classification accuracy, detection latency, robustness against disturbances, and comparative reliability across different fault types. Following the application of various fault scenarios at different feeder locations within the unbalanced IEEE 13-bus distribution system, simulation data were collected for feature analysis and classifier training. In this study, 840 samples were allocated to training, while 180 samples were used for validation and the remaining 180 samples for testing, enabling a balanced performance evaluation. Simulations were conducted using the ATP/EMTP and MATLAB/Simulink platforms, encompassing steady-state conditions, transient behaviors, and a range of LIF fault types, and Hi-ZFs. Notably, the Hi-ZF model demonstrated a nonlinear voltage-current (V–I) relationship. This nonlinearity, as illustrated in Figure 5, played a crucial role in feature extraction for accurate fault detection/classification.

A. Feature-Based Analysis for Distinguishing Hi-ZF and LIF

Figures 6(a), 6(b), 6(c), and 6(d) illustrate the maximum absolute values of current-based SDFT features for each phase namely, $SDFT_a$, $SDFT_b$, $SDFT_c$, and $SDFT_g$ under LIF and nonlinear Hi-ZF conditions. These values were analyzed at fault locations of 10 m and 50 m from

relay location (*Line 629* of 152 m length) for different fault scenario. Notably, phase (a) exhibits a marked variation in the maximum SDFT magnitude when comparing Hi-ZF and LIF conditions. This significant divergence in SDFT response, particularly in the faulty phase, confirms the effectiveness of SDFT features in capturing the distinctive spectral characteristics of each fault type. These features, when integrated with a DNN, show strong potential for enhancing fault detection, classification, and ensuring reliable discrimination between Hi-ZFs and LIFs.

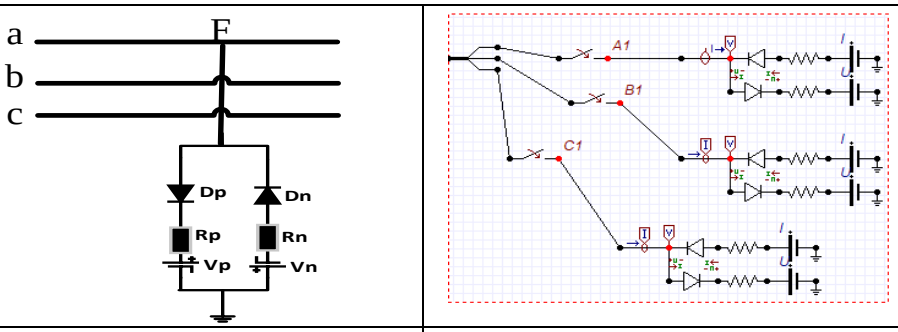

(a) Hi-ZF model [19]

(b) ATP/EMTP Hi-ZF model in sandy soil conditions

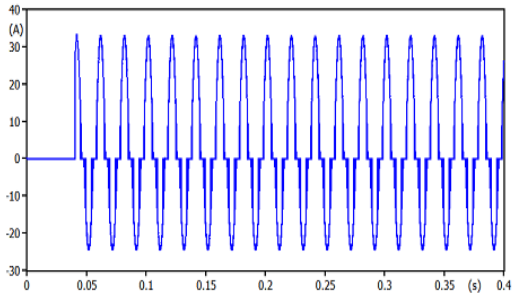

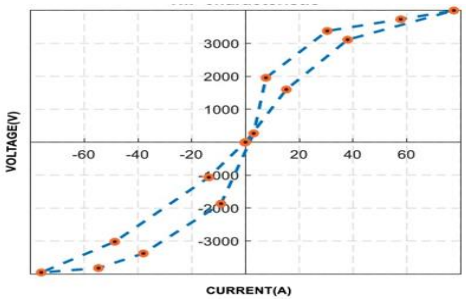

(c) Current waveform of Hi-ZF

(d) V-I Characteristics of Hi-ZF Model

Figure 5. *Hi-ZF model [19], (b) ATP/EMTP Hi-ZF model in sandy soil conditions, (c) Current waveform of Hi-ZF, (d) V-I Characteristics of Hi-ZF Model.*

B. Feature-Based Analysis for Distinguishing normal fault and no-fault conditions

Table 1 presents a comparative analysis of the maximum absolute values of current-derived SDFT features across all phases (a, b, c, and ground) along with the corresponding DNN classification outputs Line (***629***). Various conventional fault types including SLG, LL, DLG, LLL, LLL-g, and Hi-ZF, were simulated under diverse conditions such as varying inception angles, fault locations, and fault types. The results clearly validate the accuracy and reliability of the proposed scheme across all tested scenarios.

To further assess the scheme's robustness in detecting Hi-ZFs, additional simulations were conducted at the Point of Common Coupling (PCC) under a range of fault conditions throughout the low voltage distribution network. **Table 1** highlights a representative subset of the extensive test results, demonstrating that the proposed method consistently identified the fault type correctly within 26.5 ms following fault inception. Considering that the proposed scheme achieves fault detection by averaging a **25 ms** waiting time to avoid transients resulting from capacitor/load switching, or the natural imbalance present in the network under study, adding **1.5 ms** for DNN detection/classification, resulting in a precise average detection/classification time of **26.5 ms**. So, a decision is made within **26.5 ms**, ensuring prompt response for protection relays.

Moreover, various switching events such as load variations and capacitor energization were modeled to evaluate the false positive rate. In all such cases, the classifier accurately identified them as non-fault events, underscoring the scheme's immunity to typical system transients. Overall, the findings confirm that the proposed solution is highly robust to variations in fault type, location, and inception angle.

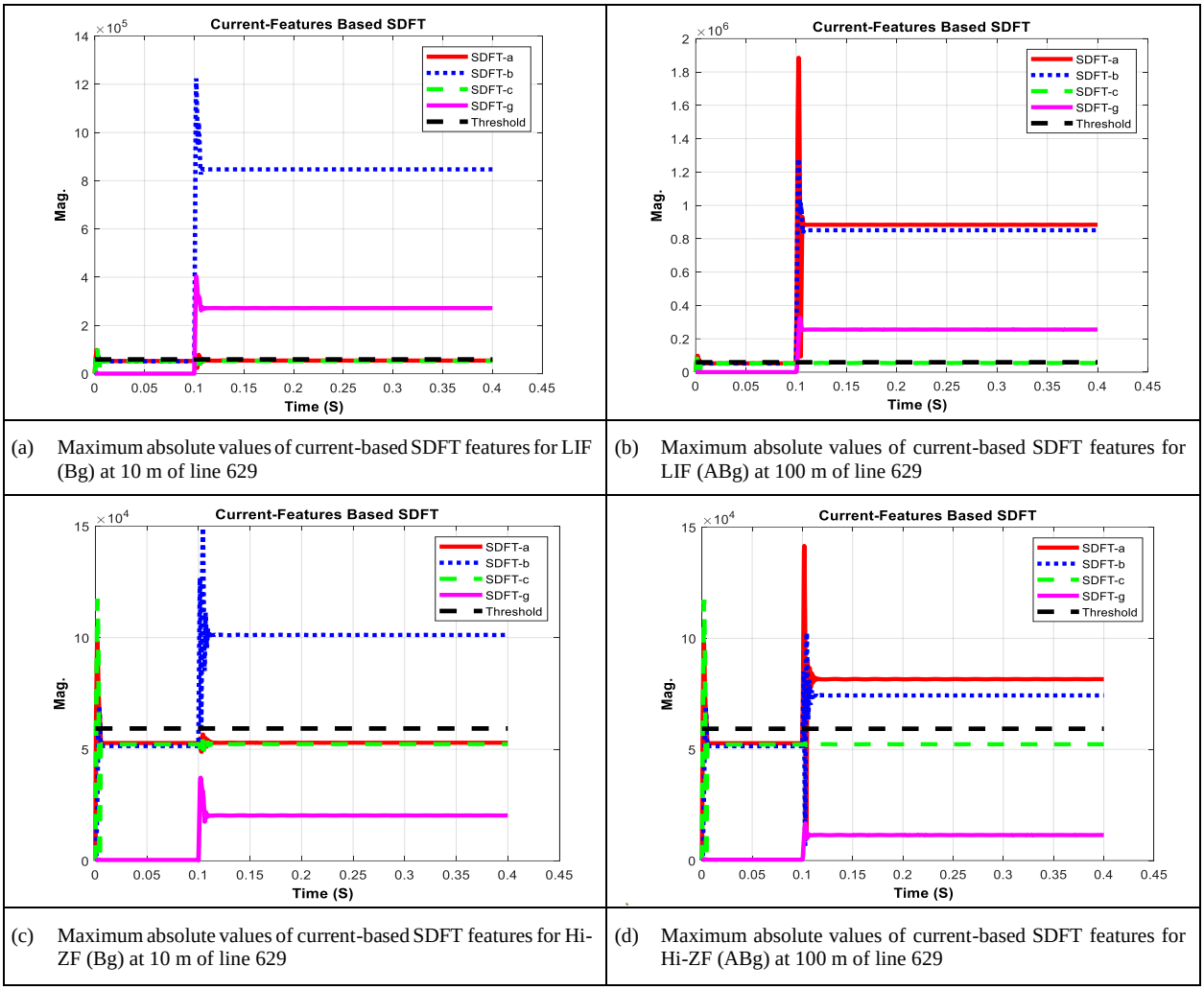

(a) Maximum absolute values of current-based SDFT features for LIF (Bg) at 10 m of line 629

(b) Maximum absolute values of current-based SDFT features for LIF (ABg) at 100 m of line 629

(c) Maximum absolute values of current-based SDFT features for Hi-ZF (Bg) at 10 m of line 629

(d) Maximum absolute values of current-based SDFT features for Hi-ZF (ABg) at 100 m of line 629

Figure 6. Current-based SDFT features for LIF and Hi-ZF (at 10 m and 100 m).

C. Classification Accuracy and General Performance

The DNN was trained and tested using a dataset generated from extensive simulations conducted on the unbalanced IEEE 13-Bus distribution feeder. The dataset included a total of 1200 samples, categorized into LIFs, Hi-ZFs, and Non-Fault Events (e.g., capacitor switching and load switching). The network achieved an overall classification accuracy of 99.1% on the test dataset. This high classification accuracy is attributed to the rich frequency-domain features extracted via SDFT, which capture the subtle distortions and waveform asymmetries associated with Hi-ZFs. These features, when coupled with the DNN's deep architecture, enable the network to learn complex, nonlinear fault signatures effectively.

TABLE 1: SAMPLES FOR SIMULATION RESULTS OF VARIOUS LIFS, HI-ZFS TYPE AND NORMAL SWITCHING CASES FOR TESTED DISTRIBUTED IEEE 13-BUS SYSTEM

Simulated case	**Line No.**	**Location (%)**	**Fault resistance (Ω)**	**Fault time occurrence, (sec)**	**The maximum absolute values of current-derived *SDFT- features***				***DNN* output for current-derived *SDFT-features***				**Event classification**
					$\lvert SDFTa\rvert \times 10^4$	$\lvert SDFTb\rvert \times 10^4$	$\lvert SDFTc\rvert \times 10^4$	$\lvert SDFTg\rvert \times 10^4$	$\lvert DNNa\rvert$	$\lvert DNNb\rvert$	$\lvert DNNc\rvert$	$\lvert DNNg\rvert$	
AG	Line (629)	5	3	0.1	**61.10**	3.60	3.89	**19.30**	1.000	0.000	0.000	1.000	**LIF-AG**
AG		95	17	0.18	**29.20**	4.11	3.70	**8.70**	1.000	0.000	0.000	1.000	**LIF-AG**
BG		8	2	0.11	3.50	**84.10**	4.06	**27.00**	0.000	1.000	0.000	1.000	**LIF-BG**
BG		40	5	0.12	3.96	**38.20**	3.72	**11.70**	0.000	1.000	0.000	1.000	**LIF-BG**
CG		5	3	0.14	3.80	3.10	**60.60**	**19.20**	0.000	0.000	1.000	1.000	**LIF-CG**
CG		50	5	0.15	4.72	3.73	**38.70**	**11.90**	0.000	0.000	1.000	1.000	**LIF-CG**
AB		5	3	0.17	**55.20**	**53.10**	3.22	0.00	1.000	1.000	0.000	0.000	**LIF-AB**
BC		40	5	0.18	3.60	**35.00**	**33.20**	0.00	0.000	1.000	1.000	0.000	**LIF-BC**
CA		96	22	0.19	**15.60**	3.59	**17.20**	0.00	1.000	0.000	1.000	0.000	**LIF-CA**
ABG		5	3	0.17	**62.50**	**60.60**	3.88	**18.50**	1.000	1.000	0.000	1.000	**LIF-ABG**
BCG		40	5	0.18	4.07	**38.70**	**39.10**	**11.50**	0.000	1.000	1.000	1.000	**LIF-BCG**
CAG		45	5	0.18	**39.50**	3.66	**39.30**	**11.70**	1.000	0.000	1.000	1.000	**LIF-CAG**
ABC		50	5	0.15	**39.80**	**39.20**	**39.60**	0.00	1.000	1.000	1.000	0.000	**LIF-ABC**
ABCg		8	2	0.17	**90.40**	**88.40**	**89.70**	**10.50**	1.000	1.000	1.000	1.000	**LIF-ABCg**
Hi-ZF-(A)		5	280	0.1	**11.60**	4.64	3.19	**6.00**	1.000	0.000	0.000	1.000	**Hi-ZF(A)**
Hi-ZF -(B)		50	280	0.15	3.70	**10.40**	3.11	**5.90**	0.000	1.000	0.000	1.000	**Hi-ZF(B)**
Hi-ZF -(C)		95	280	0.20	5.30	5.20	**12.08**	**5.93**	0.000	0.000	1.000	1.000	**Hi-ZF(C)**
Hi-ZF -(AB)		20	280	0.22	**10.60**	**10.40**	3.55	**6.50**	1.000	1.000	0.000	0.000	**Hi-ZF(AB)**
Hi-ZF -(BC)		35	280	0.22	3.70	**12.40**	**12.50**	**7.50**	0.000	1.000	1.000	0.000	**Hi-ZF(BC)**
Hi-ZF -(CA)		65	280	0.155	**11.60**	3.60	**11.60**	**5.59**	1.000	0.000	1.000	0.000	**Hi-ZF(CA)**
Cap. Sw.		50	------	0.16	4.23	3.30	3.30	0.064	0.000	0.000	0.000	0.000	**Normal Case**
Cap. Sw.		95	------	0.20	3.20	3.87	3.60	0.061	0.000	0.000	0.000	0.000	**Normal Case**
Load Sw.		5	------	0.14	3.60	3.40	3.70	0.055	0.000	0.000	0.000	0.000	**Normal Case**
Load Sw.		50	------	0.17	3.93	4.10	3.89	0.044	0.000	0.000	0.000	0.000	**Normal Case**
Base Case		15	------	0.25	3.51	3.90	4.29	0.000	0.000	0.000	0.000	0.000	**Base Case**

While the proposed method demonstrates high accuracy and acceptable detection time, its **key limitations** include reliance on simulated data, potential sensitivity to measurement noise, real-time computational challenges, and the need to validate generalization across diverse network topologies to ensure scalability and practical applicability.

Table 2 summarizes key performance results of the proposed SDFT-DNN scheme, highlighting its ability to accurately detect and classify various fault types under diverse operating and network conditions. The classifier consistently maintained high accuracy and did not falsely identify transient non-fault events as faults, demonstrating excellent noise immunity and generalization. For instance, load switching and capacitor energization commonly misclassified in rule-based systems were accurately identified as non-fault events in over **98%** of cases. Compared to conventional overcurrent relays and threshold-based Hi-ZF detection methods, the proposed scheme exhibits significant advantages:

- It does not rely on pre-defined thresholds, which are often system-specific and sensitive to noise.
- It can operate using only single-ended measurements, making it suitable for low-cost deployment.
- It successfully detects Hi-ZFs that typically evade traditional detection due to low fault current levels and nonlinear arc characteristics.

TABLE 2: SUMMARY OF KEY RESULTS	
Overall Classification Accuracy	**99.1%**
Fault Detection Time	**26.5 ms**
Precision (Hi-ZFs)	**99.18%**
Precision (LIFs)	**100%**
Accuracy under Non-Fault Events	**98.0%**
Fault Location Range Tested	10%–90%
Inception Angle Variation	0° to 330°
Fault Resistance Range	LIFs:3–50 Ω Hi-ZFs:100–280 Ω

V. CONCLUSION

This paper has introduced a robust and intelligent fault detection and classification framework for low-voltage distribution networks, leveraging a combination of Sliding Discrete Fourier Transform (SDFT) and Deep Neural Networks (DNN). The proposed approach successfully tackles the challenge of identifying both LIFs and nonlinear Hi-ZFs using only single-ended current measurements. By extracting frequency-domain features through SDFT and feeding them into a trained DNN classifier, the system achieved a high overall classification accuracy of 99.1%, demonstrated a fast response time within 26.5 ms for fault detection/classification process, and maintained excellent discrimination capability even under varying fault resistances, inception angles, and different switching conditions.

Extensive simulation studies based on the unbalanced IEEE 13-Bus test feeder confirmed the scheme's reliability and resilience in identifying fault types and distinguishing them from non-fault events such as load switching and capacitor energization. The integration of SDFT's spectral sensitivity with the pattern recognition strength of deep learning enabled accurate classification of both conventional and subtle fault events, including Hi-ZFs that are traditionally difficult to detect. The results demonstrate that the proposed ***SDFT-DNN*** framework offers a scalable and intelligent solution for modern distribution protection challenges, especially in environments where Hi-ZF detection remains a critical gap.

Future work will focus on three main directions: (i) carrying out real-time validation using actual current waveforms, (ii) integrating advanced deep learning models, such as *CNN–FWT* hybrids, to improve temporal feature extraction, and (iii) applying the framework to field data from smart grid pilot projects to confirm robustness, scalability, and practical applicability. These steps will strengthen confidence in the framework's performance under real-world operating conditions.

REFERENCES

[1] Hou, D.,2007. Detection of high-impedance faults in power distribution systems. In 2007 Power Systems Conference: Advanced Metering, Protection, Control, Communication, and Distributed Resources, pp. 85-95. IEEE. https://doi.org/10.1109/TPWRD.2006.88173.

[2] Ravaglio, Marcelo A., Luiz Felipe RB Toledo, Signie LF Santos, Luis RA Gamboa, Diogo B. Dahlke, José A. Teixeira Jr, Edson T. Yano, Alynne PM Silva, Oscar Kim Jr, and Márcio G. Antunes, 2024. Detection and location of high impedance faults in delta 13.8 kV distribution networks. Electric Power Systems Research 230: 110291.

[3] Carvalho, J. G. S., Almeida, A. R., Ferreira, D. D., Santos Jr, B. F., Vasconcelos, L. H. P., & Sobreira, D. O. 2022. High-impedance fault modeling and classification in power distribution networks. Electric Power Systems Research, 204, 107676.

[4] Cui, Q., El-Arroudi, K., & Weng, Y. 2019. A feature selection method for high impedance fault detection. IEEE Transactions on Power Delivery, 34(3), 1203-1215.

[5] Lopes, Gabriela Nunes, Vinicius Albernaz Lacerda, Jose Carlos Melo Vieira, and Denis Vinicius Coury.2020. Analysis of signal processing techniques for high impedance fault detection in distribution systems. IEEE Transactions on Power Delivery 36, no. 6: 3438-3447.

[6] Rashad, B. A. E., Ibrahim, D. K., Gilany, M. I., Abdelhamid, A. S., & Abdelfattah, W. 2024. Identification of broken conductor faults in interconnected transmission systems based on discrete wavelet transform. PloS one, 19(1), e0296773.

[7] Sarlak, M., and S. M. Shahrtash.2011. SVM-based method for high-impedance faults detection in distribution networks. COMPEL-The international journal for computation and mathematics in electrical and electronic engineering 30, no. 2: 431-450.

[8] Tiwari, Garima, and Sanju Saini. 2024. Optimizing Fault Identification in Power Distribution Systems by the Combination of SVM and Deep Learning Models." Journal of Operation and Automation in Power Engineering.

[9] Moravej, Z., & Ghahremani, M. 2023. High Impedance Fault Detection and Classification Based on Pattern Recognition. In: Zobaa, A.F., Abdel Aleem, S.H. (eds) Modernization of Electric Power Systems. Springer, Cham. https://doi.org/10.1007/978-3-031-18996-8-16

[10] Rai, K., Hojatpanah, F., Ajaei, F. B., & Grolinger, K. 2021. Deep learning for high-impedance fault detection: Convolutional autoencoders. Energies, 14(12), 3623.

[11] Abasi-obot, I. E., Kunya, A. B., Shehu, G. S., & Jibril, Y. 2023. High Impedance Fault Detection and Localization Using Fully-Connected Convolutional Neural Network: A Deep Learning Approach." Nigerian Journal of Technological Development, 20(4), 62-71.

[12] Rodrigues, L. F. A., Monteiro, H. L. M., Ferreira, D. D., Barbosa, B. H. G., Junior, C. A. R., & Duque, C. A. 2024. Sample-by-sample power quality disturbance classification based on sliding window recursive discrete fourier transform. Electric Power Systems Research, 235, 110607.

[13] S. A. Wakode, M. S. Ballal and R. R. Deshmukh, 2022. Sliding DFT-Based Fault Location Scheme for DC Microgrid. IEEE Transactions on Industry Applications, vol. 58, no. 5, pp. 5944-5954, Sept.-Oct. 2022, https://doi.org/10.1109/TIA.2022.3189610.

[14] Sozanski, Krzysztof, and Pawel Szczesniak. 2023. Advanced Control Algorithm for Three-Phase Shunt Active Power Filter Using Sliding DFT. Energies 16, no. 3: 1453. https://doi.org/10.3390/en16031453

[15] Duda, K. 2012. Accurate, guaranteed-stable, sliding DFT. Streamlining digital signal processing: A tricks of the trade guidebook, 207-214.

[16] Bramareswara Rao, S. N. V., Kumar, Y. P., Amir, M., & Muyeen, S. M. 2024. Fault detection and classification in hybrid energy-based multi-area grid-connected microgrid clusters using discrete wavelet transform with deep neural networks. Electrical Engineering, 1-18.

[17] W. H. Kersting. 1991. Radial distribution test feeders. IEEE Trans. Power Syst., vol. 6, no. 3, pp. 975–985, Aug. 1991.

[18] Samet, H., Shabanpour-Haghighi, A., and Ghanbari, T. 2017. A fault classification technique for transmission lines using an improved alienation coefficients technique. Int. Trans. Electr. Energ Syst. 27, 22355–e2323. https://doi.org/10.1002/etep.2235

[19] Gomes, D. P. S., Ozansoy, C., and Ulhaq, A. 2018. High-sensitivity vegetation high impedance fault detection based on signals high frequency contents. IEEE Trans. Power Deliv. 33 (3), 1398–1407. https://doi.org/10.1109/tpwrd.2018.2791986

[20] Ali, Z. M., Mostafa, M. H., Abdel Aleem, S. H., & Esmail, E. M. 2025. High impedance faults detection in power distribution networks using rogowski coils, kalman filtering, least-squares and non-recursive DFT computation engines. PloS one, 20(4), e0320125.

[21] Guo, M. F., Yao, M., Gao, J. H., Liu, W. L., & Lin, S. 2024. An incremental high impedance fault detection method under non-stationary environments in distribution networks. International Journal of Electrical Power & Energy Systems, 156, 109705.